LANGMUIR Article
Cite This: Langmuir 2019, 35, 13182−13188
pubs.acs.org/Langmuir

Neuromorphic Liquid Marbles with Aqueous Carbon Nanotube Cores

Richard Mayne,*[,†,‡] Thomas C. Draper,[‡] Neil Phillips,[‡] James G. H. Whiting,[§,∥,‡] Roshan Weerasekera,[§,∥] Claire Fullarton,[†,‡] Ben P. J. de Lacy Costello,[†,‡] and Andrew Adamatzky[‡]

[†]Department of Applied Sciences, Faculty of Health and Applied Sciences, [‡]Unconventional Computing Group, Faculty of the Environment and Technology, [§]Department of Engineering Design and Mathematics, Faculty of the Environment and Technology, and [∥]Health Technology Hub, University of the West of England, Frenchay Campus, Bristol BS16 1QY, U.K.

Supporting Information

ABSTRACT: Neuromorphic computing devices attempt to emulate features of biological nervous systems through mimicking the properties of synapses toward implementing the emergent properties of their counterparts, such as learning. Inspired by recent advances in the utilization of liquid marbles (LMs, microliter quantities of fluid coated in hydrophobic powder) for the creation of unconventional computing devices, we describe the development of LMs with neuromorphic properties through the use of copper coatings and 1.0 mg mL^{-1} carbon nanotube (CNT)-containing fluid cores. Experimentation was performed through sandwiching the LMs between two cup-style electrodes and stimulating them with repeated dc pulses at 3.0 V. Our results demonstrate that "entrainment" of CNT-filled copper LMs via periodic pulses can cause their electrical resistance to rapidly switch between high to low resistance profiles upon inverting the polarity of stimulation: the reduction in resistance between high and low profiles was approximately 88% after two rounds of entrainment. This effect was found to be reversible through reversion to the original stimulus polarity and was strengthened by repeated experimentation, as evidenced by a mean reduction in time to switching onset of 43%. These effects were not replicated in nanotube solutions not bound inside LMs. Our electrical characterization also reveals that nanotube-filled LMs exhibit pinched loop hysteresis IV profiles consistent with the description of memristors. We conclude by discussing the applications of this technology to the development of unconventional computing devices and the study of emergent characteristics in biological neural tissue.

1. INTRODUCTION

Computation is a ubiquitous property of natural matter that, through a universal and objective language, will unite the sciences. More generally, physical systems may be applied to mathematical problems to create machines and computers. Complex systems may be correspondingly abstracted in algorithmic terms in order to describe phenomena that have traditionally evaded the grasp of understanding, such as complexity arising from biological sensorial-actuation networks, through which phenomena such as "intelligence" are hypothesized to emerge,[1−7] even in organisms that do not possess nervous systems.[8] This application of computing concepts and development of experimental devices therein encompasses the field of "unconventional computing".

A neuromorphic characteristic of an engineered system is so named if it mimics the structure or functionality of a component/multiple components of the metazoan nervous system. Typically, this will involve attempts to replicate the phenomenon of synaptic plasticity: self-modulation of the impedance of neuron−neuron junctions (synapses) toward replicating state retention ("learning") via a process of entrainment (phase synchronization) with graduated input ("neuromodulation"). Neuromorphic devices are worthy of research attention as an unconventional computing paradigm due to certain features of their biological counterparts—such as massive parallelism, emergence, and low energy consumption[9,10]—being highly desirable to emulate.

This article aims to create neuromorphic computing devices from liquid marbles (LMs). LMs are spherical microliter quantities of fluid with a superhydrophobic particulate coating, which can range in size between tens and thousands of micrometers in diameter.[11−14] These systems exhibit novel characteristics such as low coefficients of friction,[15−17] which have been exploited by nature.[18,19] It has been demonstrated that LMs have myriad uses including microreactors,[14,20−23] gas biosensors,[24,25] and unconventional computing media.[26,27] LMs are responsive to various forms of stimuli, which can be used to control various characteristics such as coalescence, shape, and wetting.[28] Our laboratory has developed LM devices that are capable of implementing computation through a variety of nonstandard logics[26,27,29] where the LMs are considered as data, or otherwise to contain data (i.e., chemical reactants), which may interact with other LMs via collisions that will result in data translation or transfer via ricochets or coalescence. Toward these

Received: August 15, 2019
Revised: September 16, 2019
Published: September 17, 2019

goals, we (and others) have also examined LM dynamics to enhance their usefulness for these purposes, for example, evaporation[30,31] and ballistic interactions.[32,33] The current work is therefore presented as a route toward developing microliter-quantity three-dimensional ballistic-chemical reactors that exhibit neuromorphic properties and may hence be used as unconventional computing media.

The first liquid-state neuromorphic devices to be demonstrated were composed of UV-curable zinc oxide polymers;[34] for our LMs however, the liquid core chosen was an aqueous dispersion of carbon nanotubes (CNTs). In 2001 Cui et al.[35] experimentally demonstrated that single walled-CNTs can be switched between two conductance states (high-conductance and low-conductance), which differ by more than 2 orders of magnitude, with a threshold voltage shift of 1.25 V. Theoretical analysis has shown that CNTs can act as Schottky barrier transistors[36] and several patent applications for CNT switching devices have been filed.[37,38] Regarding progress toward implementations of CNT computing systems, field effect transistors have been described,[39] and experimental laboratory evidence suggests that the solid-state switching signatures of CNTs might be due to their relative mechanical movements.[40] CNT artificial synapses have previously been prototyped separately by K. Kim et al.[41] and S. Kim et al.:[42] the synapse operates via dynamic interactions between CNTs and hydrogen ions in an electrochemical cell integrated in the synapse. Our aim was to capitalize on these properties of CNTs within LMs.

The following article is structured as follows: first, we present our methods for producing neuromorphic LMs, using a copper coating and a CNT-containing solution core. After presenting our results, which detail the electrical characterization of our LMs, including descriptions of entrainment protocols, we proceed to discuss their design, putative uses, and present limitations.

2. EXPERIMENTAL SECTION

LMs were prepared using copper flakes (Goodfellow, UK) (average diameter 76 μm, n = 838) and 100 μL of liquid droplets. Copper flakes of this variety, which have substantial surface roughness, have been previously demonstrated to be sufficiently hydrophobic for generating LMs.[43] Upon gentle contact of the liquid with the bed of copper flakes, spontaneous LM formation was observed; the copper flakes migrated around the droplet of liquid, forming a completely coated LM without the need of rolling (this phenomenon has been previously observed using ethanol/water binary solutions and hydrophobized glass beads,[44] as well as with copper flakes[43]). The experimental LM fluid core was a single-walled CNT dispersion at 1 mg mL^{-1}, in deionized water (DIW) containing 1% (w/v) Triton X-100 (CHASM Advanced Materials, USA). Addition of the surfactant Triton has been demonstrated to maintain complete dispersion of CNTs in aqueous solutions.[45] CNT dimensions were approximately 20 nm diameter and over 1 μm length. Typical electron microscopical appearances of the materials used are shown in Figure 1 (see the Supporting Information for preparation details).

CNT solutions were sonicated prior to use for 10 min. Control LMs were prepared using DIW (15 MΩ cm) cores. Attempts were made to fabricate control LMs using 1% Triton X-100 in DIW, but the surfactant nature of the additive in the absence of hydrophobic CNTs prevented LMs from forming. Previous reports using Triton X-100 (even with a more hydrophobic powder coating) also had limited success forming stable LMs at this concentration.[46] Care was taken to ascertain, both before and after experiments, that LMs had not wetted either electrode surface.

LMs were subject to electrical characterization via two cup-style Ag/AgCl electrodes (Figure 2a,b), each with a total end-to-end resistance not exceeding 0.5 Ω. One electrode was placed concavity-side up and

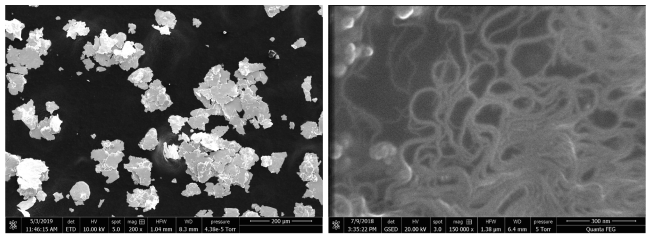

(a) (b)

Figure 1. Scanning electron micrographs of the experimental materials used. (a) Copper flakes, which were used for LM coatings. (b) CNTs, used in LM cores.

the LMs were rolled into the depression. The second electrode, mounted to a clamp stand, was then lowered onto the LM. The electrode spacing was assessed by eye to compress the LM slightly, at an interelectrode gap of 2.0−2.5 mm, which ensured that the upper surface of the LMs remained in contact with the upper electrode in the event of LM deformation. These electrodes were chosen for their shape rather than their electrical properties, hence, a brief series of replicate experiments were performed using flat copper plates instead of the cup electrodes, each measuring 10 × 10 × 1.0 mm, to ascertain that the results observed were indeed a function of the sample, rather than the electrode material.

No steps were undertaken to prevent fluid evaporation from the LM because (a) a focus of our investigation was evolution of LM characteristics over time in standard room temperature and humidity conditions and (b) our previous work[30] has demonstrated that the effects of evaporation over the experiment duration (50 min) is likely to have been negligible.

Electrical measurements were made via a Keithley source measure unit (SMU) 2450 (Keithley Instruments, USA), using a 4-to-2 electrode setup. A current limit of 100 mA was used throughout. The principal experiment involved repeatedly stimulating the LM using a 3.0 V pulse (0.5 s ramp time, hence 1.0 s per pulse), followed by a delay (i.e. 0 V) of the same duration. This stimulation pattern of 0 → 3 V was repeated 375 times per "phase", each phase therefore lasting 750 s. Furthermore, a second stimulation phase was started which was identical to the first, except for polarity being switched to −3.0 V. This overall pattern was repeated, that is 375 pulses at 3.0 V, then 375 pulses at −3.0 V, twice, such that each experiment's duration was 3000 s. These four phases are here named $s_1 \rightarrow s_4$. The stimulus voltage was greater than the thermodynamic requirement for the hydrolysis of water and, one would suspect, also high enough to overcome the inherent kinetic barrier. However, perhaps because of the inverting pulsed nature of our experiment, no obvious hydrolysis was observed.

All experiments were repeated 10 times. Pulse frequency, duration, and magnitude were all chosen as the result of prior testing, toward designing experiments where minimal voltages were used in order to reduce breakdown of water products while keeping experiments short enough to reduce the impact of fluid evaporation from marbles. For completeness, IV sweeps were also conducted with the same instrument using a 3 V double-sided sweep, 0.1 s dwell time with a 0.1 A current limit.

Further control measurements were also collected on 100 μL samples of fluids (dispersed CNTs and solvated Triton X-100 in DIW, Triton X-100 in DIW, both at the same concentrations as previously stated, and pure DIW), henceforth referred to as "free liquid" (FL) experiments. This was achieved through the use of bespoke circuit boards developed in our laboratory for bulk electrical testing of fluid samples, connected to the same measurement apparatus described above (Figure 2c). Full details of these boards' design and fabrication are included in the Supporting Information.

All analyses were performed using MATLAB 2017a (MathWorks, USA). All datasets were found to be normally distributed via Shapiro−Wilk tests ($p < 0.01$ in all instances) and hence further investigation into effect size was not conducted. Each experiment (CNT LMs, water LMs and water, Triton X-100 and CNT FL experiments) was repeated 10

DOI: 10.1021/acs.langmuir.9b02552
Langmuir 2019, 35, 13182−13188

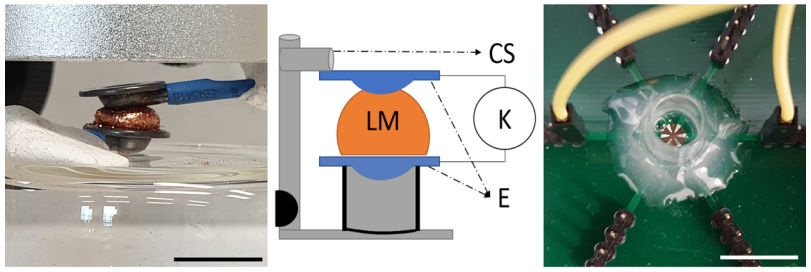

Figure 2. Experimental electrical recording apparatus. (a) LM recording apparatus. Two 10 mm$^{\phi}$ Ag/AgCl cup electrodes were used to "sandwich" LMs, with an electrode spacing of 2.0−2.5 mm. Scale bar 5 mm. (b) Schematic diagram of LM recording apparatus (not to scale). CS: clamp stand; LM: liquid marble; K: Keithley SMU; E: electrodes. (c) Fluids were placed into wells overlying needle-shaped electrodes; only one pair of electrodes were used in the experiments described here. Scale bar 10 mm.

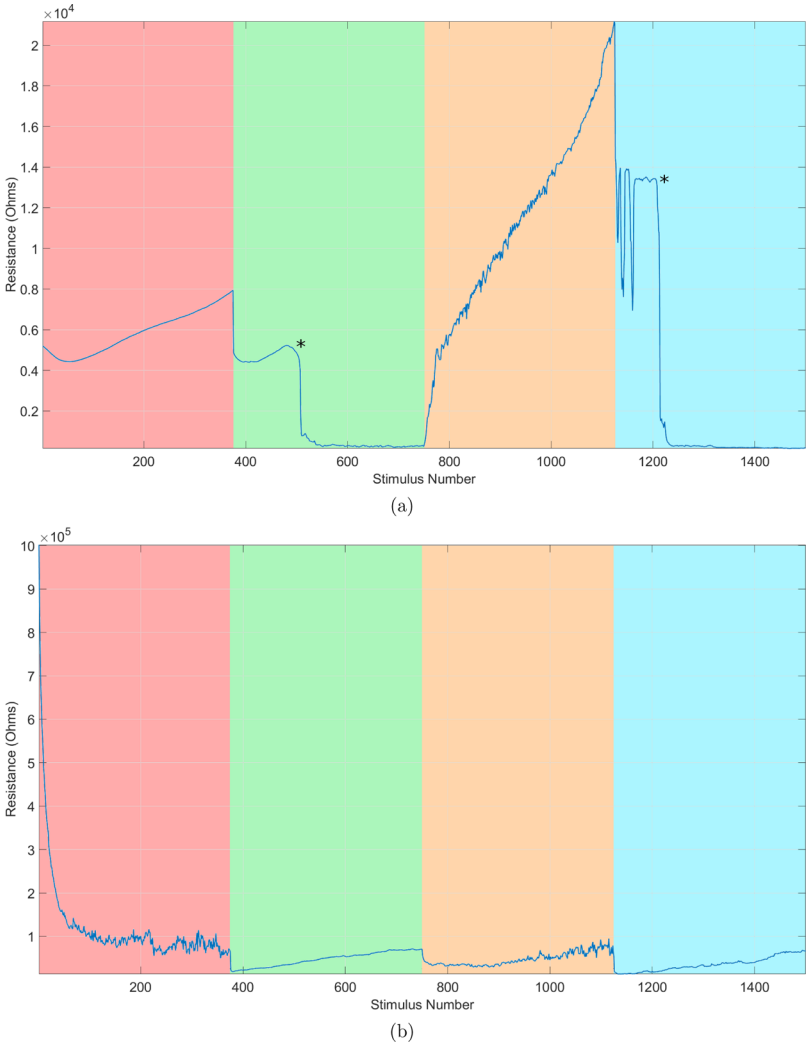

Figure 3. Graphs to illustrate typical resistance of LMs exposed to 3 V pulses at periodically alternating polarities. Colored areas indicate stimulation phases (red for s_1, green for s_2, orange for s_3 and blue for s_4) and resistance values at 0 V have been omitted for clarity. (a) CNT LM, showing NSEs (asterisks). (b) Control water-filled LM. No NSEs are visible.

times, except for IV sweeps and copper electrode tests, where $n = 5$. All varieties of statistical tests used were two-tailed.

3. RESULTS AND DISCUSSION

3.1. Description of Neuromorphic Property. An emergent characteristic was observed in LMs filled with the CNT solution that will henceforth be known as a "neuromorphic switching effect" (NSE), the characteristics of which were as follows (Figure 3a). Repeated stimulation with 3 V pulses during s_1 caused CNT-filled LMs to maintain a high-resistance state (quantitative data are presented in subsection 3.2), during which fluctuations in their electrical properties were minor. The switching of polarity during s_2 resulted in the LM initially assuming a similar profile as during s_1, before suddenly switching

DOI: 10.1021/acs.langmuir.9b02552
Langmuir 2019, 35, 13182−13188

to a more conductive profile. The majority of LMs experienced drops in resistance of 1 to 2 orders of magnitude during s_2. Entering phase s_3 (reverting to the original polarity), the LMs were observed to briefly retain their lower resistance profile before rapidly dropping back to a high resistance profile, similar to those observed in s_1. After a final polarity change during s_4, the LMs were observed to return to their low resistance profile. The LMs invariably switched to their low resistance profile in a shorter time period than during s_2.

It is noteworthy that an NSE was not observed in the water-filled control LMs (Figure 3b) or in any of the FL experiments. The NSE was observed in CNT-filled LMs sandwiched between copper (rather than Ag/AgCl) electrodes, but not in water-filled LMs or any variety of FL when tested with copper electrodes. For example datasets, see the Supporting Information.

3.2. Characteriztion of Neuromorphic System Effect. Differences in mean resistance of CNT-filled LMs between phases $s_1 \rightarrow s_4$ were found to be significant through analysis of variance (ANOVA) (Table 1). There was also a significant difference in mean resistances of CNTs in FL between these phases, although NSEs were not observed in these experiments. No significant difference between means between phases was observed in any other sample type. The resistance of CNT LMs was subject to a large degree of variation [which ranged from 5.67 to 46.3 kΩ (mean 46.6 kΩ) in unstimulated s_1 CNT LMs and 0.05−19.3 kΩ (mean 3.15 kΩ) in s_4 CNT LMs], likely resulting from inconsistent contact areas between LMs and their top electrodes, hence data on conductivity changes are here presented as percentage changes in resistance between phases (Table 2). Percentage differences in mean resistance between phases $s_1 \rightarrow s_2$ and $s_1 \rightarrow s_4$ were found to be significant, with variation reducing markedly in the latter measurement.

Table 1. Table To Show ANOVA Results, Comparing Differences in Means between Phases in LMs Containing CNTs and Water, in Addition to FL Controls Containing CNTs, Triton X-100 (T), and Water[a]

	CNT LM	H_2O LM	CNT FL	T FL	H_2O FL
F	3.236	1.086	3.490	0.700	1.970
p	0.035[b]	0.392	0.041[b]	0.561	0.137

[a]*F*: *F*-statistic, *p*: *p*-value. [b]$p < 0.05$.

Table 2. Table To Show One-Sample *t*-Test Results, Comparing Percentage Changes in Resistance between $s_1 \rightarrow s_2$, $s_1 \rightarrow s_4$, and $s_2 \rightarrow s_4$ in LMs Containing CNTs[a]

	mean PC	med PC	CI low	CI high	SD	*p*
$s_1 \rightarrow s_2$	63.95	97.64	22.18	105.7	58.40	0.007[b]
$s_1 \rightarrow s_4$	87.70	98.48	71.58	103.8	22.53	0.000[c]
$s_2 \rightarrow s_4$	29.23	38.67	−13.82	72.27	60.17	0.159

[a]CI: confidence interval (in %), Med: median (in %), PC: percentage change (in %), SD: standard deviation. [b]$p < 0.05$. [c]$p < 0.0001$.

This raises the question as to whether CNT LM resistance drops further in s_4 than in s_2. Although approximately 60% of CNT LMs demonstrated a subsequent reduction in resistance s_4 from the values they exhibited during s_2, the remainder either continued to reproduce similar resistances or a slightly increased resistance, hence a significant difference in percentage change between $s_2 \rightarrow s_4$ was not observed.

The time to NSE onset during phases s_2 and s_4 was also investigated. Similarly to the CNT LM's resistance, onset times were highly variable, ranging from 11 to 309 s, mean 84.8 s during s_2 and 4−106 s, mean 41.8 s during s_4. It was observed that the longer time to NSE onset correlated with datasets with a higher overall resistance, hence, this phenomenon was reasoned to also be linked to LM−electrode contact area. When measured as a percentage difference in onset between s_2 and s_4, it was found that the difference between time to onset was significantly shorter between s_2 and s_4 (Table 3).

Table 3. Table To Show Two-Sample *t*-Test Results, Comparing Percentage Changes in Mean NSE Onset Time between Phases s_2 and s_4 in LMs Containing CNTs[a]

	mean PC	med PC	SD	*p*
$s_2 \rightarrow s_4$	43.20	39.73	22.75	0.0005[b]

[a]CI: confidence interval (in %), Med: median (in %), PC: percentage change (in %), SD: standard deviation [b]$p < 0.01$.

3.3. CNT LM IV Profile. A typical IV profile for a previously unstimulated CNT LM is shown in Figure 4. Allowing for the LMs saturating at the instrument current limit when exposed to a continuous dc source, all samples ($n = 5$) were observed to produce a pinched-loop hysteresis, consistent with the description of a memristive device.[47]

3.4. Further Discussion. We have described here laboratory experimental work in which we generated LMs which exhibit the neuromorphic properties of: (1) switching between two distinct electrochemical states in response to excitatory or inhibitory electrical input signals; (2) potentiation, that is, an increase in signal in response to repeated dc pulses ("training"); and (3) memory of previous states, as evidenced by a reduced time to NSE and IV profiles consistent with descriptions of memristors. We propose, therefore, that CNT LMs may be considered as soft nonbiological synapses. Although CNTs have been successfully used as components of LM cores before,[48] to our knowledge, this is the first published description of a neuromorphic LM.

We did not observe any incidence of the NSE in CNT FL experiments, although as there was a statistically significant difference in mean resistance between phases, we are not discounting the possibility that this may still occur with alternate testing parameters. Regardless of whether this effect is a function purely of CNTs or otherwise, the NSE has specific applications when packaged within a LM. Although copper has been described as a LM coating material before,[43] its significance in enabling the NSE is unclear and will form the topic of future work.

Although the mechanisms underlying the NSE in CNT LMs were not elucidated with the experiments detailed here, significant work has been done on the electrical properties of CNTs and their propensity to align according to electromagnetic fields is well-established.[49] Furthermore, many neuromorphic devices based on CNT technologies have been proposed and work has begun on implanting CNTs into biological neurons, the effects of which appear to include neuromodulation.[50]

Previous authors have studied the effects of charging of CNTs in response to electrical stimulation, which could likely underlie the phenomena observed in this study.[51−53] This is also somewhat consistent with results on CNTs sustaining and promoting neuronal electrical activity in networks of cultured cells as reported by Cellot et al.,[50] where it is proposed that the

DOI: 10.1021/acs.langmuir.9b02552
Langmuir 2019, 35, 13182−13188

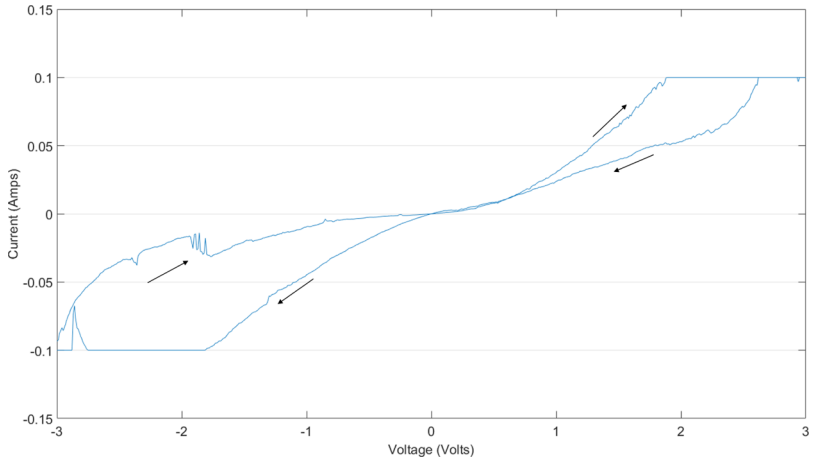

Figure 4. Graph to show a typical IV sweep profile from a CNT LM exposed to a 3 V double-ended sweep. Arrows indicate sweep direction.

reported effects could be due to clustering of CNTs and the resulting close contact with the neural membrane. We discuss hypothetical mechanisms underlying the NSE in the Supporting Information.

Switching behavior may be used as the basis for computing circuitry, including logic gates and bistables: this would be the most facile route toward producing CNT LM computing devices. When considering their neuromorphic characteristics, however, even a single memristive device which exhibits spiking behavior may be capable of implementing combinatorial logic operations (e.g., full adders) when device I/O operations are sequence-sensitive.[54,55] It is therefore clear that more refined methods are available to enhance the viability of CNT LMs as unconventional computing media.

The benefits to our devices being encapsulated within LMs are manifold[12,13] but revolve around their representing soft, ballistic data sources whose contents may be considered as chemical reactors. Through the exploitation of principles of collision-based computing,[56] LM computing devices may be used to implement nonstandard, "collision-based" conservative logics.[26] Integration of LM features such as collisions whose outcome may be engineered (reflection or coalescence) and the potential for chemical reactions between two heterogenous fluid cores following collision, further enhances the toolbox of traditional conservative logic. The applications of such a device include enhancing our understanding of the nervous system and hence information processing in mammals, control of adaptable and autonomous liquid robots,[57] and various lab-on-a-chip applications.

Our future work on neuromorphic LMs will establish the number of stimuli and switching cycles necessary to produce an NSE, their longevity under these conditions, and how consistent memory effects are over time. Further work on elucidating the mechanism underlying the phenomena described here will also be prioritized.

4. CONCLUSIONS

Key characteristics of CNT LMs are as follows.

1. Sensitization of the LM and/or their contents causes a rapid drop in resistance shortly after inverting the polarity of stimulation (the NSE).
2. Repeated stimulation across multiple phases causes a more reliable and more stable decrease in LM resistance, which may be equated with the concept of training.
3. Repeated stimulation across multiple phases causes the NSE to occur more rapidly, which may also be equated with training.

We propose that this technology is of interest to the design and fabrication of massively parallel wet computers whose applications range from computing to biomedicine.

■ ASSOCIATED CONTENT

Supporting Information

The Supporting Information is available free of charge on the ACS Publications website at DOI: 10.1021/acs.langmuir.9b02552.

Overview of the Hex PBC design used in FL experiments, typical datasets for control experiments, electron microscopy of LM materials, and the hypothetical model for neuromorphic effect (PDF)

■ AUTHOR INFORMATION

Corresponding Author

*E-mail: richard.mayne@uwe.ac.uk.

ORCID

Richard Mayne: 0000-0003-1915-4993

Notes

The authors declare no competing financial interest.

■ ACKNOWLEDGMENTS

The authors thank Dr. David Patton and Sue Hula, of the Department of Applied Sciences at UWE Bristol, for their expertise with the scanning electron microscope. T.C.D., C.F., B.P.J.d.L.C., and A.A. acknowledge support of EPSRC with grant EP/P016677/1.

■ REFERENCES

(1) Priel, A.; Tuszynski, J. A.; Woolf, N. J. *J. Biol. Phys.* **2010**, *36*, 3−21.

(2) Mayne, R.; Adamatzky, A.; Jones, J. On the role of the plasmodial cytoskeleton in facilitating intelligent behavior in slime mold Physarum polycephalum. *Commun. Integr. Biol.* **2015**, *8*, No. e1059007.

(3) Adamatzky, A.; Mayne, R. *Int. J. Bifurcation Chaos* **2015**, *25*, 1550030.

(4) Mayne, R.; Adamatzky, A. The Physarum polycephalum actin network: formalisation, topology and morphological correlates with computational ability. *8th International Conference on Bio-Inspired Information and Communications Technologies (Formerly BIONETICS)*, 2014; pp 87−94.

DOI: 10.1021/acs.langmuir.9b02552
Langmuir 2019, 35, 13182−13188

(5) Woolf, N.; Priel, A.; Tuszyński, J. In *Nanoneuroscience. Structural and Functional Roles of the Neuronal Cytoskeleton in Health and Disease*; Woolf, N., Priel, A., Tuszynski, J., Eds.; Springer: Berlin, 2010; pp 85−127.
(6) Hameroff, S. R. *Ultimate Computing*; North-Holland: Amsterdam, 1987.
(7) Lahoz-Beltra, R.; Hameroff, S. R.; Dayhoff, J. E. Cytoskeletal logic: a model for molecular computation via Boolean operations in microtubules and microtubule-associated proteins. *BioSystems* **1993**, *29*, 1−23.
(8) Whiting, J. G. H.; Jones, J.; Bull, L.; Levin, M.; Adamatzky, A. *Sci. Rep.* **2016**, *6*, 19948.
(9) Stepney, S. The neglected pillar of material computation. *Phys. D* **2008**, *237*, 1157−1164.
(10) Sengupta, B.; Stemmler, M. B. Power Consumption During Neuronal Computation. *Proc. IEEE* **2014**, *102*, 738−750.
(11) Aussillous, P.; Quéré, D. Liquid marbles. *Nature* **2001**, *411*, 924.
(12) McHale, G.; Newton, M. I. Liquid marbles: principles and applications. *Soft Matter* **2011**, *7*, 5473.
(13) McHale, G.; Newton, M. I. Liquid marbles: topical context within soft matter and recent progress. *Soft Matter* **2015**, *11*, 2530−2546.
(14) Bormashenko, E. Liquid Marbles, Elastic Nonstick Droplets: From Minireactors to Self-Propulsion. *Langmuir* **2017**, *33*, 663−669.
(15) Aussillous, P.; Quéré, D. Properties of liquid marbles. *Proc. R. Soc. A* **2006**, *462*, 973−999.
(16) Bormashenko, E.; Bormashenko, Y.; Musin, A.; Barkay, Z. On the Mechanism of Floating and Sliding of Liquid Marbles. *ChemPhysChem* **2009**, *10*, 654−656.
(17) Bormashenko, E.; Bormashenko, Y.; Oleg, G. On the Nature of the Friction between Nonstick Droplets and Solid Substrates. *Langmuir* **2010**, *26*, 12479−12482.
(18) Pike, N.; Richard, D.; Foster, W.; Mahadevan, L. How aphids lose their marbles. *Proc. R. Soc. London, Ser. B* **2002**, *269*, 1211−1215.
(19) Kasahara, M.; Akimoto, S.-i.; Hariyama, T.; Takaku, Y.; Yusa, S.-i.; Okada, S.; Nakajima, K.; Hirai, T.; Mayama, H.; Okada, S.; Deguchi, S.; Nakamura, Y.; Fujii, S. Liquid Marbles in Nature: Craft of Aphids for Survival. *Langmuir* **2019**, *35*, 6169−6178.
(20) Bormashenko, E. Liquid marbles: Properties and applications. *Curr. Opin. Colloid Interface Sci.* **2011**, *16*, 266−271.
(21) Fullarton, C.; Draper, T. C.; Phillips, N.; de Lacy Costello, B. P. J.; Adamatzky, A. Belousov-Zhabotinsky reaction in liquid marbles. *J. Phys. Mater.* **2019**, *2*, 015005.
(22) Ooi, C. H.; Nguyen, N.-T. Manipulation of liquid marbles. *Microfluid. Nanofluid.* **2015**, *19*, 483−495.
(23) Oliveira, N. M.; Reis, R. L.; Mano, J. F. The Potential of Liquid Marbles for Biomedical Applications: A Critical Review. *Adv. Healthcare Mater.* **2017**, *6*, 1700192.
(24) Tian, J.; Arbatan, T.; Li, X.; Shen, W. Liquid marble for gas sensing. *Chem. Commun.* **2010**, *46*, 4734.
(25) Tian, J.; Arbatan, T.; Li, X.; Shen, W. Porous liquid marble shell offers possibilities for gas detection and gas reactions. *Chem. Eng. J.* **2010**, *165*, 347−353.
(26) Draper, T. C.; Fullarton, C.; Phillips, N.; de Lacy Costello, B. P. J.; Adamatzky, A. Liquid marble interaction gate for collision-based computing. *Mater. Today* **2017**, *20*, 561−568.
(27) Draper, T. C.; Fullarton, C.; Phillips, N.; de Lacy Costello, B. P. J.; Adamatzky, A. *Sci. Rep.* **2018**, *8*, 14153.
(28) Fujii, S.; Yusa, S.-i.; Nakamura, Y. Stimuli-Responsive Liquid Marbles: Controlling Structure, Shape, Stability, and Motion. *Adv. Funct. Mater.* **2016**, *26*, 7206−7223.
(29) Draper, T. C.; Fullarton, C.; Phillips, N.; de Lacy Costello, B. P. J.; Adamatzky, A. In *UCNC 2018, LNCS 10867*; Stepney, S., Verlan, S., Eds.; Springer, 2018; pp 59−71.
(30) Fullarton, C.; Draper, T. C.; Phillips, N.; Mayne, R.; De Lacy Costello, B. P. J.; Adamatzky, A. *Langmuir* **2018**, *34*, 2573.
(31) Dandan, M.; Erbil, H. Y. Evaporation Rate of Graphite Liquid Marbles: Comparison with Water Droplets. *Langmuir* **2009**, *25*, 8362−8367.
(32) Draper, T. C.; Fullarton, C.; Mayne, R.; Phillips, N.; Canciani, G. E.; de Lacy Costello, B. P. J.; Adamatzky, A. Mapping outcomes of liquid marble collisions. *Soft Matter* **2019**, *15*, 3541−3551.
(33) Planchette, C.; Biance, A.-L.; Pitois, O.; Lorenceau, E. Coalescence of armored interface under impact. *Phys. Fluids* **2013**, *25*, 042104.
(34) Chiolerio, A.; Roppolo, I.; Bejtka, K.; Asvarov, A.; Pirri, C. F. Resistive hysteresis in flexible nanocomposites and colloidal suspensions: interfacial coupling mechanism unveiled. *RSC Adv.* **2016**, *6*, 56661−56667.
(35) Cui, J. B.; Sordan, R.; Burghard, M.; Kern, K. Carbon nanotube memory devices of high charge storage stability. *Appl. Phys. Lett.* **2002**, *81*, 3260−3262.
(36) Heinze, S.; Tersoff, J.; Martel, R.; Derycke, V.; Appenzeller, J.; Avouris, P. *Phys. Rev. Lett.* **2002**, *89*, 106801.
(37) Bertin, C. L.; Rueckes, T.; Segal, B. M. Nanotube-based switching elements with multiple controls. U.S. Patent 6,990,009 B2, 2006.
(38) Choi, W.-b.; Yoo, I.-k.; Chu, J.-u. Memory device utilizing carbon nanotubes. U.S. Patent 7,015,500 B2, 2006.
(39) Avouris, P. Molecular Electronics with Carbon Nanotubes. *Acc. Chem. Res.* **2002**, *35*, 1026−1034.
(40) Diehl, M. R.; Steuerman, D. W.; Tseng, H.-R.; Vignon, S. A.; Star, A.; Celestre, P. C.; Stoddart, J. F.; Heath, J. R. Single-Walled Carbon Nanotube Based Molecular Switch Tunnel Junctions. *ChemPhysChem* **2003**, *4*, 1335−1339.
(41) Kim, K.; Chen, C.-L.; Truong, Q.; Shen, A. M.; Chen, Y. A Carbon Nanotube Synapse with Dynamic Logic and Learning. *Adv. Mater.* **2013**, *25*, 1693−1698.
(42) Kim, S.; Choi, B.; Lim, M.; Yoon, J.; Lee, J.; Kim, H.-D.; Choi, S.-J. Pattern Recognition Using Carbon Nanotube Synaptic Transistors with an Adjustable Weight Update Protocol. *ACS Nano* **2017**, *11*, 2814−2822.
(43) Chang, C.-C.; Wu, C.-J.; Sheng, Y.-J.; Tsao, H.-K. Spontaneous self-coating of a water drop by flaky copper powders: critical role of the particle shape. *Soft Matter* **2015**, *11*, 4469−4475.
(44) Whitby, C. P.; Bian, X.; Sedev, R. Spontaneous liquid marble formation on packed porous beds. *Soft Matter* **2012**, *8*, 11336.
(45) Keinänen, P.; Siljander, S.; Koivula, M.; Sethi, J.; Sarlin, E.; Vuorinen, J.; Kanerva, M. *Heliyon* **2018**, *4*, No. e00787.
(46) Wang, C.; He, Y. Timed disintegrating of the liquid marbles containing triton X-100. *Colloids Surf., A* **2018**, *558*, 367−372.
(47) Biolek, D.; Biolkova, V.; Kolka, Z. Memristor pinched hysteresis loops: Touching points, Part I. 2014. *International Conference on Applied Electronics*, 2014; pp 37−40.
(48) Nakai, K.; Nakagawa, H.; Kuroda, K.; Fujii, S.; Nakamura, Y.; Yusa, S.-i. Near-infrared-responsive Liquid Marbles Stabilized with Carbon Nanotubes. *Chem. Lett.* **2013**, *42*, 719−721.
(49) Sun, X.; Chen, T.; Yang, Z.; Peng, H. The Alignment of Carbon Nanotubes: An Effective Route To Extend Their Excellent Properties to Macroscopic Scale. *Acc. Chem. Res.* **2013**, *46*, 539−549.
(50) Cellot, G.; Cilia, E.; Cipollone, S.; Rancic, V.; Sucapane, A.; Giordani, S.; Gambazzi, L.; Markram, H.; Grandolfo, M.; Scaini, D.; Gelain, F.; Casalis, L.; Prato, M.; Giugliano, M.; Ballerini, L. Carbon nanotubes might improve neuronal performance by favouring electrical shortcuts. *Nat. Nanotechnol.* **2009**, *4*, 126.
(51) Poncharal, P.; Wang, Z. L.; Ugarte, D.; De Heer, W. A. Electrostatic Deflections and Electromechanical Resonances of Carbon Nanotubes. *Science* **1999**, *283*, 1513−1516.
(52) Maciel, I. O.; Anderson, N.; Pimenta, M. A.; Hartschuh, A.; Qian, H.; Terrones, M.; Terrones, H.; Campos-Delgado, J.; Rao, A. M.; Novotny, L.; Jorio, A. Electron and phonon renormalization near charged defects in carbon nanotubes. *Nat. Mater.* **2008**, *7*, 878.
(53) Matsunaga, R.; Matsuda, K.; Kanemitsu, Y. *Phys. Rev. Lett.* **2011**, *106*, 037404.
(54) Gale, E. M. Neuromorphic computation with spiking memristors: habituation, experimental instantiation of logic gates and a novel sequence-sensitive perceptron model. *Faraday Discuss.* **2019**, *213*, 521−551.

DOI: 10.1021/acs.langmuir.9b02552
Langmuir 2019, 35, 13182−13188

(55) Diederich, N.; Bartsch, T.; Kohlstedt, H.; Ziegler, M. *Sci. Rep.* **2018**, *8*, 9367.
(56) *Collision-Based Computing*; Adamatzky, A., Ed.; Springer-Verlag: London, 2002.
(57) Chiolerio, A.; Quadrelli, M. B. Smart Fluid Systems: The Advent of Autonomous Liquid Robotics. *Adv. Sci.* **2017**, *4*, 1700036.

DOI: 10.1021/acs.langmuir.9b02552
Langmuir 2019, 35, 13182−13188